International Journal of Electrical and Electronic Engineering & Telecommunications

ISSN 2319 – 2518 www.ijeetc.com
Vol. 5, No. 3, July 2016

Research Paper

SHUNT CONNECTED HYBRID ACTIVE POWER FILTERS BY USING DC-LINK VOLTAGE CONTROLLER

Vaisali[1]* and P D V S K Kishore[2]

*Corresponding Author: Vaisali, ✉ vaisali.eee205@gmail.com

Active filters are widely used in power system for reactive power compensation and voltage/ current harmonic elimination. Harmonic contents of the source current has been calculated and compared for the different cases to demonstrate the influence of harmonic extraction circuit on the harmonic compensation characteristic of the shunt active power filter. In this paper, a fuzzy logic controlled, three-phase shunt active filter is used to improve power quality by compensating current harmonics which is required by a nonlinear load. However, when the LC-HAPF is performing dynamic reactive power compensation, this dc-link voltage control scheme will influence the reactive power compensation, and thus, makes the LC-HAPF lack of success to carry out dynamic reactive power compensation. In this paper, a novel dc-link voltage control scheme for LC-HAPF is proposed so that the dc-link voltage control with start-up self-charging process can be obtained as well as providing dynamic reactive power compensation. Representative simulation and experimental results of the three-phase four-wire center-spilt LC-HAPF are presented to verify all deductions, and also show the effectiveness of the proposed dc-link voltage control scheme in dynamic reactive power compensation.

Keywords: Active Power Filters (APFs), dc-link voltage control, Hybrid Active Power Filters (HAPFs), Passive Power Filters (PPFs), Reactive power control

INTRODUCTION

In this modern society, domestic customers' appliances nor-mally draw large harmonic and reactive current from the sys-tem. High harmonic current causes various problems in power systems and consumer products, such as overheating in equip-ment and transformer, blown capacitor fuses, excessive neutral current, low power factor, etc. (Subjek and Mcquilkin, 1990; and Duarte and Alves, 2002). On the other hand, load-ings with low power factor draw more reactive current than those with high power factor. The larger the reactive current/power, the larger the system current losses and lower the network stability.

[1] Student, EEE Department, Narasaraopeta Engineering College, Narasaraopeta, India.

[2] Assistant Professor, EEE Department, Narasaraopeta Engineering College, Narasaraopeta, India.

Thus, electrical utilities usually charge the industrial and com-mercial customers a higher electricity cost with a low power factor situation.

To eliminate the harmonic and reactive current problems, application of power filters is one of the most suitable solutions. Since the first installation of Passive Power Filters (PPFs) in the mid 1940s, PPFs have been widely used to suppress harmonic current and compensate reactive power in distribution power systems (Senini and Wolfs, 2002) due to their low-cost, simplicity, and high-efficiency characteristics. However, they have many disadvantages such as low dynamic performance, filtering characteristics easily be affected by small variations of the system parameter values and resonance problems.

Since the concept "active ac power filter" was first devel-oped by Gyugyi in 1976 the research studies of the Active Power Filters (APFs) for current quality compensation have been prospered since then. Although APFs overcome the disadvantages inherent in PPFs, the initial and operational costs are relatively high due to its high dc-link operating voltage during inductive loading. This results in slowing down their large-scale applications in distribution networks.

Later on, different Hybrid APF (HAPF) topologies composed of active and passive parts in series and/or parallel have been pro-posed, in which the active part is a controllable power electronic converter, and the passive part is formed by *RLC* component. This combination aims to improve the compensation character-istics of PPFs and reduces the voltage and/or current ratings (costs) of the APFs, thus providing a cost-effective solution for compensating reactive and harmonic current problems (Peng *et al.*, 1990; Fujita and Akagi, 1991; Akagi, 1996; Park *et al.*, 1999; Fujita *et al.*, 2000; Rivas *et al.*, 2003; Srianthumrong and Akagi, 2003; Inzunza and Akagi, 2005; Tangtheerajaroonwong *et al.*, 2007; Jou *et al.*, 2008; Luo *et al.*, 2009a, 2009b and 2009c; Rahmani *et al.*, 2009; and Salmerón and Litrán, 2010). Among HAPF topologies in Peng *et al.* (1990), Fujita and Akagi (1991), Akagi (1996), Park *et al.* (1999), Fujita *et al.* (2000), Rivas *et al.* (2003), Luo *et al.* (2009a, 2009b and 2009c) and Salmerón and Litrán (2010), a transformerless *LC* cou-pling HAPF (*LC*-HAPF) has been proposed and applied recently for current quality compensation and damping of harmonic propagation in distribution power system, in which it has less passive components and lower dc-link operating volt-age comparing with an APF.

In addition, *LC*-HAPF is normally designed to deal with harmonic current rather than reactive power compensation, the inverter part is responsible to compensate har-monic currents only and the passive part provides a fixed amount of reactive power. In practical case, the load-side reactive power consumption usually varies from time to time, and if the load-ing mainly consists of induction motors such as centralized an air-conditioning system, its reactive power consumption will be much higher than the harmonic power consumption (Tai *et al.*, 2007). As a result, it is necessary for the *LC*-HAPF to perform dynamic reactive power compensation together with harmonic current compensation.

All *LC*-HAPF and other HAPFs discussed in Peng *et al.* (1990), Fujita and Akagi (1991), Akagi (1996), Park *et al.* (1999), Fujita *et al.*

(2000), Rivas *et al.* (2003), Srianthumrong and Akagi (2003), Inzunza and Akagi (2005), Tangtheerajaroonwong *et al.* (2007), Jou *et al.* (2008), Luo *et al.* (2009a, 2009b and 2009c), Rahmani *et al.* (2009) and Salmerón and Litrán (2010) are based on fixed dc-link voltage reference. For the purpose of reducing switching loss and switching noise, an adaptive dc-link voltage reference control is proposed in Lam *et al.* (2012). However, the au-thor did not discuss the dc-link voltage control in details and also the inherent influence between the reactive power compen-sation and dc-link voltage controls. Moreover, this influence has not been discussed.

Due to the limitations among the existing literatures, this pa-per aims to investigate and explore different dc-link voltage con-trol techniques for the three-phase four-wire *LC*-HAPF while performing dynamic reactive power compensation:

1) By using the traditional dc-link voltage control scheme as an active current component, an extra start-up dc-link precharging control process is necessary.
2) To achieve the start-up dc-link voltage self-charging func-tion, a dc-link voltage control as a reactive current com-ponent for the *LC*-HAPF is proposed (Cui *et al.*, 2011); however, the *LC*-HAPF with this dc-link voltage control scheme fails to provide dynamic reactive power compensation.
3) A novel dc-link voltage control method is proposed for achieving start-up dc-link self-charging function, dc-link voltage control, and dynamic reactive power compensation. Moreover, the proposed method can be applied for the adaptive dc-link voltage reference control as discussed in Lam *et al.* (2012).

In this paper, the designed coupling *LC* is based on the aver-age value of the loading reactive power consumption, while the designed dc-link voltage level is based on the *LC*-HAPF maximum reactive power compensation range specification. Therefore, even though the reactive power compensating range is small with a low dc-link voltage, the *LC*-HAPF can still provide dynamic reactive power compensation. Thus, its reactive power compensation ability (within its specification) is still effective. Given that most of the loads in the distribution power systems are inductive, the following analysis and discussion will only focus on inductive loads (Lam *et al.*, 2008).

A TRANSFORMERLESS TWO-LEVEL THREE-PHASE FOUR-WIRE CENTER-SPILT LC-HAPF

Circuit Structure of LC-HAPF

The circuit structure of a transformerless three-phase four-wire center-spilt *LC*-HAPF is shown in Figure 1, where subscript "*x*" denotes phases *a, b, c,* and *n*. *vsx* is the source voltage, v_x is the load voltage, L_s is the source inductor and normally neglected due to its low value relatively; thus, v_{sx}"—,v_x· i_{sx}, i_{Lx}, and i_{cx} are the source, load, and compensating current for each phase. C_c and L_c are the coupling part capacitor and inductor for each leg of the converter. C_{dcU}, C_{dcL}, V_{dcU}, and V_{dcL} are the upper and lower dc-link capacitor and dc-link capacitor voltages, and the dc-link voltage $V_{dc} = V_{dcU} + V_{dcL}$. Since the transformerless two-level three-phase four-wire center-spilt *LC*-HAPF can be treated as three independent

Figure 1: Circuit Structure of a Transformerless Three-Phase Four-Wire Center-Spilt LC-HAPF

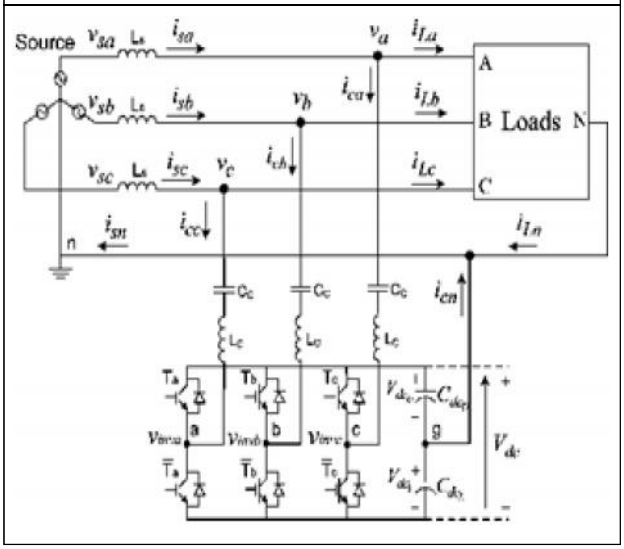

Figure 2: Single-Phase Equivalent Circuit Model of a Three-Phase Four-Wire Center-Spilt LC-HAPF

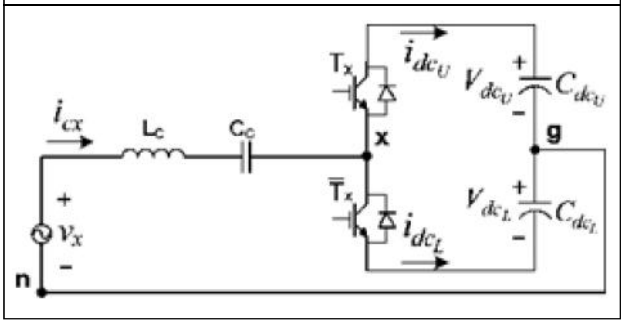

single-phase circuits, its single-phase equivalent circuit model is shown in Figure 2.

Modeling of the DC-Link Voltage in a LC-HAPF Single-Phase Equivalent Circuit

From Figure 2, the compensating current *icx* can flow either C_{dcU} or C_{dcL} and returns through the neutral wire in both directions of Insulated-Gate Bipolar Transistors (IGBT) switches. The dc-link capacitor voltages can be expressed as

$$V_{dcU} = \frac{1}{C_{dcU}} \int i_{dcU}\, dt \qquad V_{dcL} = -\frac{1}{C_{dcL}} \int i_{dcL}\, dt \quad ...(1)$$

where i_{dcU} and i_{dcL} are the dc currents of upper and lower dc-link capacitors, respectively, and

$$i_{dcU} = s_x i_{cx},\ i_{dcL} = (1 - s_x) i_{cx} \quad ...(2)$$

Substituting (2) into (1), the completed upper and lower dc capacitor voltages V_{dcU} and V_{dcL} become

$$V_{dcU} = \frac{1}{C_{dcU}} \int s_x i_{cx}\, dt$$

$$V_{dcL} = -\frac{1}{C_{dcL}} \int i(1 - s_x) i_{cx}\, dt \quad ...(3)$$

$$s_x = \begin{cases} 1, & \text{if } T_x = 1 \quad T_x = 0 \\ 0, & \text{if } T_x = 0 \quad \overline{T_x} = 1 \end{cases} \quad ...(4)$$

In (3) and (4), *sx* represents the switching function of one inverter leg in *x* phase based on the hysteresis current Pulse Width Modulation (PWM) method, and that is the binary state of the upper and lower switches (T_x and T_x). When the positive di-rection of i_{cx} is assumed as Figure 2, the switching logic for each phase is formulated as Singh and Verma (2005): if $i_{cx} > (i^{*}cx + hb)$, T_x is ON and T_x is OFF, then $s_x = 1$; if $icx < (i^{*}cx - hb)$, T_x is OFF and T_x is ON, then $s_x = 0$, where i^{*}_{cx} is the reference compensating current and *hb* is the width of the hysteresis band.

According to the mathematical model in (3), if compensat-ing current $i_{cx} > 0$, the upper dc-link voltage V_{dcU} is increased during switching function $s_x = 1$, while the lower dc-link voltage *V*dc*L* is decreased for $s_x = 0$. The inverse results can be obtained if $i_{cx} < 0$. Figure 3 shows the operation of a single-phase voltage source inverter under different switching modes by using hysteresis current PWM method (Aredes *et al.*, 1997). The changes of the upper and lower dc-link voltages V_{dcU} and

Figure 3: Operation of a Single-Phase Voltage Source Inverter Under Different Switching Modes by Using Hysteresis Current PWM Method

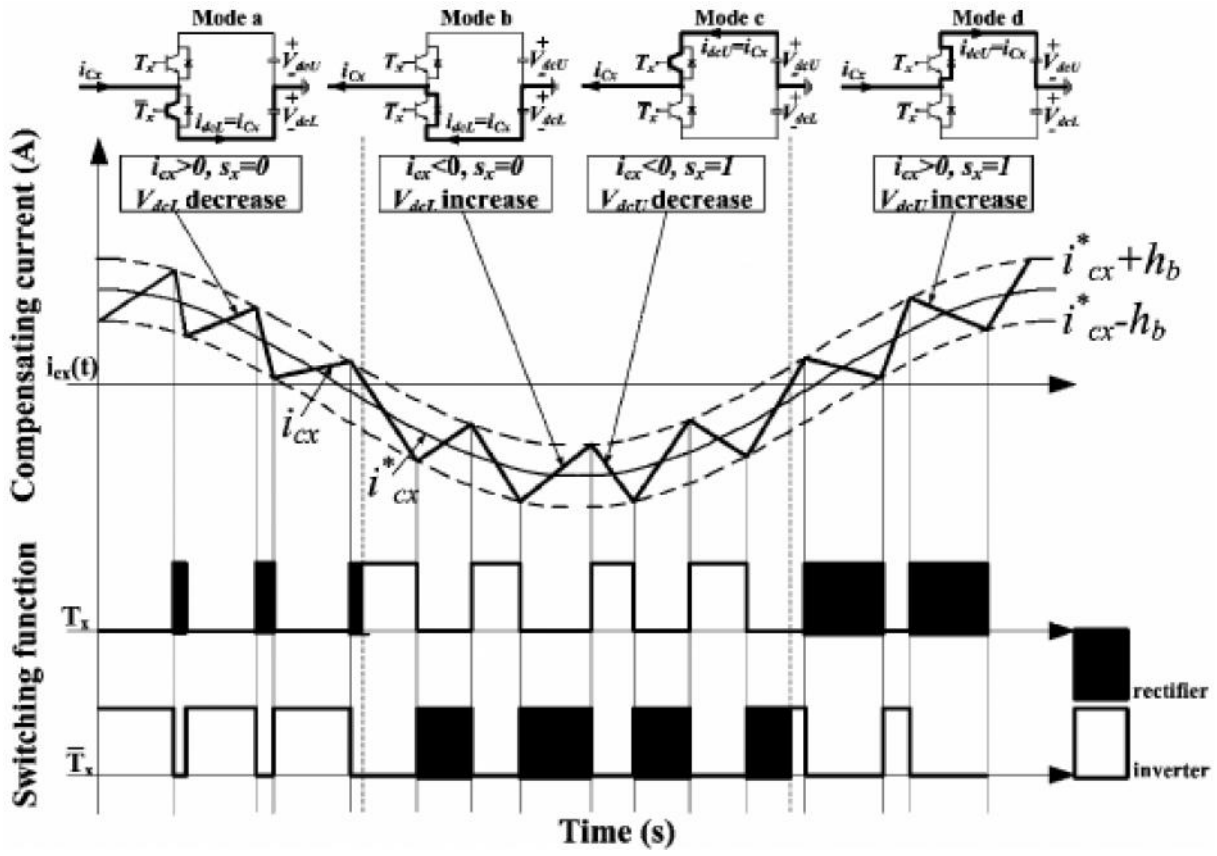

Table 1: The Change of the Capacitor Voltages (V_{dcU}, V_{dcL}) Under Different Modes

Switching mode	i_{cx} conditions	Switching function	Operating circuit	Change of dc capacitor voltage
a	$i_{cx}>0$	$s_x=0, T_x=0, \overline{T_x}=1$	Inverter	V_{dcL} decrease
b	$i_{cx}<0$	$s_x=0, T_x=0, \overline{T_x}=1$	Rectifier	V_{dcL} increase
c	$i_{cx}<0$	$s_x=1, T_x=1, \overline{T_x}=0$	Inverter	V_{dcU} decrease
d	$i_{cx}>0$	$s_x=1, T_x=1, \overline{T_x}=0$	Rectifier	V_{dcU} increase

V_{dcL} under different modes are summarized in Table 1.

INFLUENCE ON DC-LINK VOLTAGE DURING LC-HAPF PERFORMS REACTIVE POWER COMPENSATION

This section aims to present and analyze the influence on the dc-link voltage when *LC*-HAPF performs reactive power compensation. Through this analysis, the dc-link capacitor voltage will either be increased or decreased during fundamental reactive power compensation under insufficient dc-link

voltage. Moreover, the influence is proportional to the difference between the *LC*-HAPF compensating current *icx* and its pure reactive reference $i^{*}_{cxf\,q}$, where the subscript "*f*," "*p*," and "*q*" denote fundamental, active, and reactive components.

Reactive Power Compensation Under Sufficient DC-Link Voltage

Under sufficient dc-link voltage, the compensating current generated by the *LC*-HAPF i_{cx} can track its pure reactive refer-ence $i^{*}_{cxf\,q}$, as shown in Figure 4, thus the amplitude $I^{*}_{cxfq} \approx I_{cx}$. Provided that the hysteresis band is small enough for the *LC*-HAPF to be operated at linear region, the PWM switching function in (4) will be evenly distributed, as shown in Figure 4. According to Table 1, the *LC*-HAPF will be changed between the operating modes of rectifier and inverter (modes a, b, c, and d), and keeping the average dc-link voltage as a constant. In ideal lossless case, the dc-link voltage will not be affected when *LC*-HAPF performs reactive power compensation during

$I_{cxfq} \approx I_{cx}$ case.

Reactive Power Compensation Under Insufficient DC-Link Voltage

Under insufficient dc-link voltage, the compensating reactive current generated by the *LC*-HAPF i_{cx} cannot track its pure reactive reference i^{*}_{cxfq}, in which there are two possible situations: 1) If the amplitude $I_{cx} > I^{*}_{cxfq}$; thus, the instantaneous relationship gives $i_{cx} > i^{*}_{cxfq}$ during $i_{cx} > 0$, and $i_{cx} < i^{*}_{cxfq}$ during $i_{cx} < 0$, as shown in Figure 5; 2) If the amplitude $I_{cx} < I^{*}_{cxfq}$, the opposite instantaneous relationship is given as shown in Figure 6.

Hence, to force the compensating current i_{cx} to track its reference i_{cxfq} correspondingly:

- For $I_{cx} > I^{*}_{cxfq}$ case, as shown in Figure 5, when the hystere sis band is relatively small

Figure 4: i_{cx} and i^{*}_{cxfq} during $i_{cx} \approx i^{*}_{cxfq}$ Case and the Corresponding Switching Function

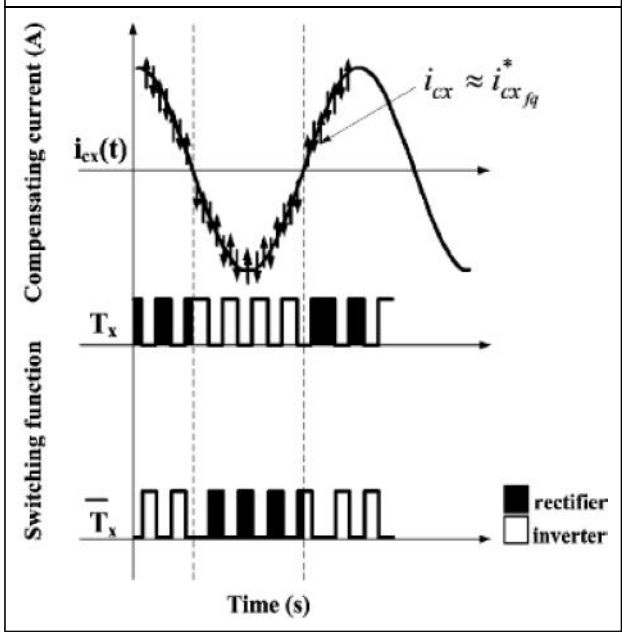

Figure 5: i_{cx} and i^{*}_{cxfq} During $i_{cx} > i^{*}_{cxfq}$ Case and the Corresponding Switching Function

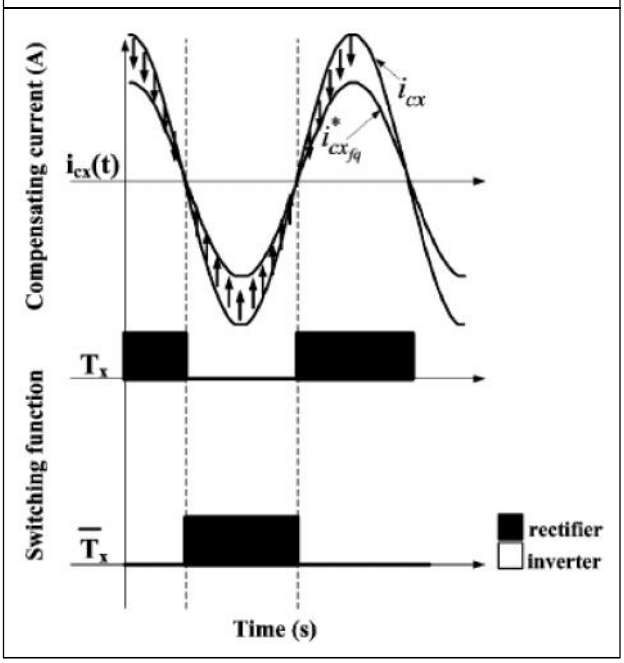

Figure 6: i_{cx} and i^*_{cxfq} During $i_{cx} < i^*_{cxfq}$ Case and the Corresponding Switching Function

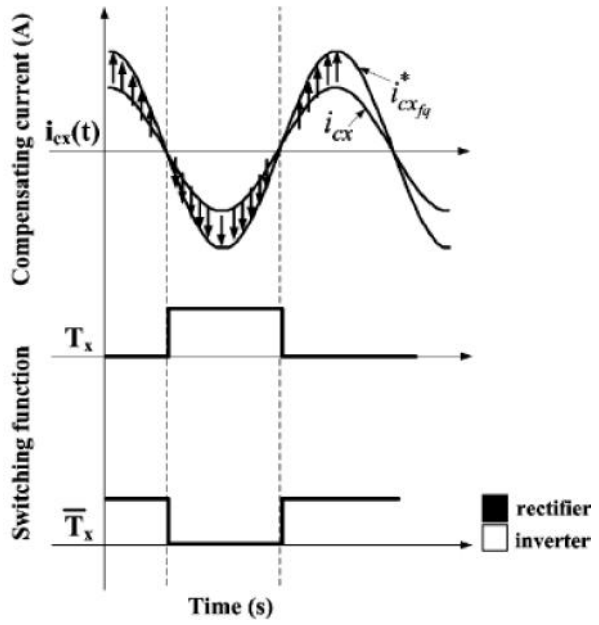

compared with the difference between i_{cx} and i^*_{cxfq}, their instantaneous relationship between i_{cx} and i^*_{cxfq} can be expressed as follows:

$$i_{cx} > (i^*_{cx_{fq}} + h_b) \quad \text{for } i_{cx} > 0 \qquad ...(5)$$

$$i_{cx} < (i^*_{cx_{fq}} - h_b) \quad \text{for } i_{cx} < 0 \qquad ...(6)$$

Based on the hysteresis PWM technique, the switching functions of (5) and (6) are

$$s_x = 1(T_x = 1, \overline{T_x} = 0) \quad \text{for } i_{cx} > 0 \qquad ...(7)$$

$$s_x = 0(T_x = 0, \overline{T_x} = 1) \quad \text{for } i_{cx} < 0 \qquad ...(8)$$

According to Table 1, the PWM switching sequences in (7) and (8) drive the *LC*-HAPF to be operated in rectifier mode (modes b and d), thus increasing the average dc-link capacitor voltage. When the dc-link voltage is increased to sufficient high level, the *LC*-HAPF will change the operating mode from $I_{cx} > I^*_{cxfq}$ into $I_{cx} \approx I^*_{cxfq}$, and keeping the dc-link voltage value. Therefore, for a given fundamental reactive current ref-erence i^*_{cxfq} ($I_{cx} > I^*_{cxfq}$), the dc-link voltage of *LC*-HAPF will be self-increased to a voltage level that lets the reference compensating current can be tracked.

For $I_{cx} < I^*_{cxfq}$ case, as shown in Figure 6, the instantaneous relationship between i_{cx} and i^*_{cxfq} is

$$i_{cx} < (i^*_{cx_{fq}} + h_b) \quad \text{for } i_{cx} > 0 \qquad ...(9)$$

$$i_{cx} > (i^*_{cx_{fq}} - h_b) \quad \text{for } i_{cx} < 0 \qquad ...(10)$$

The switching functions of (9) and (10) are

$$s_x = 0(T_x = 0, \overline{T_x} = 1) \quad \text{for } i_{cx} > 0 \qquad ...(11)$$

$$s_x - 1(T_x - 1, \overline{T_x} - 0) \quad \text{for } i_{cx} < 0 \qquad ...(12)$$

According to Table 1, the PWM switching sequences in (11) and (12) drive the *LC*-HAPF to be operated in inverter mode (modes a and c), thus decreasing the average dc-link capacitor voltage.

LC-HAPF OPERATION BY CONVENTIONAL DC-LINK VOLTAGE CONTROL METHODS

DC-Link Voltage Control Method as Active Current Component

Traditionally, if the indirect current (voltage reference) PWM control method is applied, the dc-link voltage of the inverter is controlled by the reactive current component feedback signal. However, when the direct current PWM control method is applied in the dc-link voltage should be controlled by the active current component feedback signal. Both dc-link voltage control methods are equivalent to each other.

When *LC*-HAPF performs reactive power

compensating, the reference compensating current i^*_{cx} is composed by

$$i^*_{cx} - i^*_{cx_{fq}} + i^*_{cx_{fp\_dc}} - i^*_{Lx_{fq}} + i^*_{cx_{fp\_dc}} \quad ...(13)$$

However, to perform the reactive power and dc-link voltage control action in (13), a sufficient dc-link voltage should be provided to let the compensating current *icx* track with its reference i^*_{cx}. As a result, this conventional dc-link voltage control method fails to control the dc-link voltage during insufficient dc-link voltage, such as during start-up process. Due to this reason, when this dc-link voltage control method is applied in *LC*-HAPF, an extra start-up precharging control process is nec-essary. Usually, a three-phase uncontrollable rectifier is used to supply the initial dc-link voltage before operation. Moreover, when the adaptive dc-link voltage control idea is ap-plied, the reference dc-link voltage may be changed from a low level to a high level; at that occasion, the dc-link voltage may be insufficient to track the new reference value. Therefore, the conventional dc-link voltage control with precharging method may not work properly in the adaptive dc-link voltage controlled system.

The *LC*-HAPF in showed that this dc-link voltage control can achieve start-up self-charging function without any external supply. That is actually due to the *LC*-HAPF in which is initially operating at *Icx* > *I***cxf q* condition. According to the analysis in Section III, during $I_{cx} > I^*_{cxfq}$ condition, the dc-link voltage will be self-charging to a sufficient voltage level that lets the *LC*-HAPF's compensating current track with its reference $i^*_{cxfq} \approx i_{cx}$. Thus, the dc-link voltage can be maintained as its reference value in steady state. However, if the *LC*-HAPF is initially operating at $I_{cx} < I^*_{xfq}$ condition, this dc-link voltage control method fails *c* to carry out this function.

Figures 7 and 8 show the simulation results of *LC*-HAPF start-up process by using the conventional dc-link voltage control method under different cases. From Figure 7, when *LC*-HAPF starts operation during $I_{cx} > I^*_{cxfq}$ condition, the dc-link voltage *V*dc can carry out the start-up self-charging function and $i^*_{cx} \approx i_{cx}$ in steady state. On the contrary, from Figure 8, neither the dc-link voltage nor the reactive power compensa-tion can be controlled when *LC*-HAPF is operating during $I_{cx} < I^*_{cxfq}$ condition, in which the simulation results verified the previous analysis.

DC-Link Voltage Control Method as Reactive Current Component

According to the analysis in Section III, the dc-link voltage can be influenced by varying the reference compensating fundamental reactive current i^*_{cxfq} under insufficient dc-link voltage; thus, the dc-link voltage can also be controlled

Figure 7: V_{dc}, i^*_{cx}, and i_{cx} During $I_{cx} > I^*_{cxfq}$ Condition with Conventional dc-Link Voltage Control Method as Active Current Component

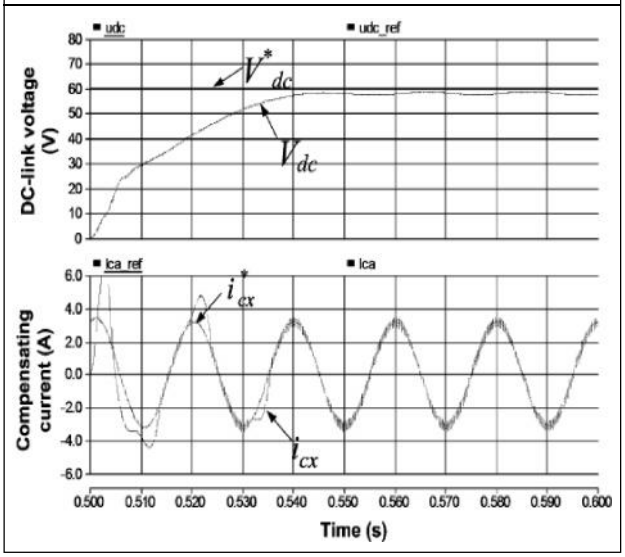

Figure 8: V_{dc}, i^*_{cx}, and i_{cx} During $I_{cx} < I^*_{cxfq}$ Condition with Conventional dc-Link Voltage Control Method as Active Current Component

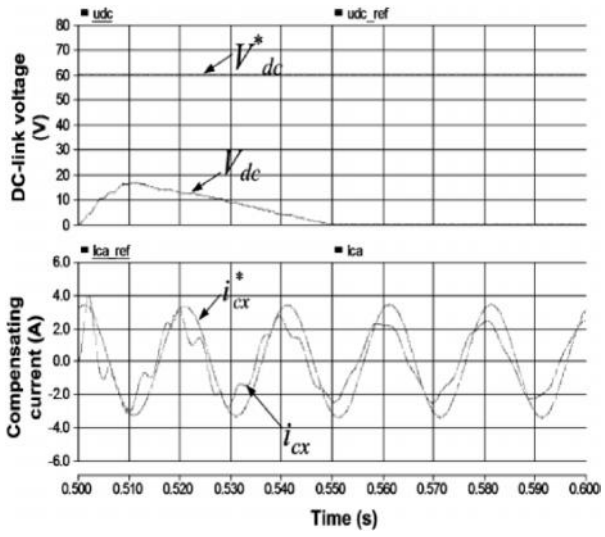

by utilizing this influence. Hence, this dc-link voltage control method can achieve the start-up self-charging function. Moreover, it has been shown that this method is more effective than that conventional method as active current component. However, when it is being applied in *LC*-HAPF, although the dc-link voltage can be controlled as its reference value, the *LC*-HAPF cannot perform dynamic reactive power compensation. The corresponding reason can be derived as follows.

By using the dc-link voltage control method as reactive current component, the reference compensating current i^*_{cx} is composed by

$$i^*_{cx} = i^*_{cx_{fq}} = i^*_{Lx_{fq}} + i^*_{cx_{fq}\_dc} \quad ...(14)$$

where i^*_{cxfq} dc is the dc-link voltage control signal related to reactive current component.

Based on the analysis in Section III, under insufficient dc-link voltage, the change of the dc-link voltage is directly proportional to the difference between the amplitude of I_{cx} and I^*_{cxfq}. Moreover, it has been concluded that for a given reference i^*_{cxfq}($I_{cx} > I^*_{cxfq}$), the dc-link voltage will be self-charging to a voltage level, then i_{cx} can trend its reference i^*_{cxfq} gradually, and maintaining this voltage level in steady state. Therefore, to control the dc-link voltage Vdc as its reference V^*_{dc}, it will have a corresponding fixed reference value, that is, $I^*_{cxfq} = I^*_{cxfq}$ fixed.

Therefore

$$V^*_{\mathrm{dc}}|_{I^*_{cx_{fq}} = I^*_{cx_{fq}\_\mathrm{fixed}}} - V_{\mathrm{dc}} = 0 \quad ...(15)$$

Equation (15) implies that to control the dc-link voltage, the *LC*-HAPF must restrict to provide a fixed amount of reactive power. Therefore, by using the dc-link voltage control method as reactive current component, the *LC*-HAPF fails to perform dynamic reactive power compensation, in which the corresponding simulation and experimental results will be given in Section VI.

PROPOSED DC-LINK VOLTAGE CONTROL METHOD

From the previous analysis, the dc-link voltage control method as active current component is effective only under sufficient dc-link voltage. In an insufficient dc-link voltage case, such as the *LC*-HAPF start-up process, both dc-link voltage control and reactive power compensation may fail. On the contrary, when the dc-link voltage control method as reactive current component is applied, the dc-link voltage control can be effectively controlled with start-up self-charging function. However, by using this control method, the *LC*-HAPF fails to perform dynamic reactive power compensation. As a result, a novel dc-link voltage control method by both reactive and

active current components as the feedback signals is proposed in this section, so as to combine the advantages of both methods, which can achieve the start-up self-charging function, dc-link voltage control, and dynamic reactive power compensation.

$$\Delta Q_{\mathrm{dc}} = -k_q \cdot (V^*_{\mathrm{dc}} - V_{\mathrm{dc}}) \quad ...(16)$$

$$\Delta P_{\mathrm{dc}} = k_p \cdot (V^*_{\mathrm{dc}} - V_{\mathrm{dc}}) \quad ...(17)$$

where ΔQ_{dc} and ΔP_{dc} are the dc control signals related to the reactive and active current components and k_q and k_p are the corresponding positive gains of the controller. By using the proposed control method, the reference compensating current i^*_{cx} is calculated by

$$i^*_{cx} = i^*_{cx_{fq}} + i^*_{cx_{fp\_\mathrm{dc}}} \quad ...(18)$$

where $i^* = i^*L_{xfq} + i^*$

cxfqcxf q d c.

In (17), ΔP_{dc} represents the active power flow between the source and the LC-HAPF compensator, $\Delta P_{dc} > 0$ means the LC-HAPF absorbs active power from the source, and $\Delta P_{dc} < 0$ means the LC-HAPF injects active power to the source. According to the analysis in Section III, the dc-link voltage will be charged for $I_{cx} > I^*_{cxfq}$, and discharged for $I_{cx} < I^*_{cxfq}$ during performing reactive power compensation. When $V^*_{dc} - V_{dc} > 0$, in order to increase the dc-link voltage, I^*_{cxfq} should be decreased by adding a negative ΔQ_{dc}. On the contrary, when $V^*_{dc} - V_{dc} < 0$, in order to decrease the dc-link voltage, I^*_{cxfq} should be increased by adding a positive ΔQdc. Therefore, the "_" sign is added in (16). In this paper, in order to simplify the control process, ΔQ_{dc} and ΔP_{dc} in (16) and (17) are calculated by the same controller, i.e., $k_q = k_p$.

In (18), i^*_{Lxfq}, i^*_{cxfq} dc and i^*_{cxfp} dc are calculated by using the three-phase instantaneous $p - q$ theory

$$\begin{bmatrix} i^*_{La_{fq}} \\ i^*_{Lb_{fq}} \\ i^*_{Lc_{fq}} \end{bmatrix} = \sqrt{\frac{2}{3}} \times \frac{1}{v_0 v^2_{\alpha\beta}} \begin{bmatrix} 1/\sqrt{2} & 1 & 0 \\ 1/\sqrt{2} & -1/2 & \sqrt{3}/2 \\ 1/\sqrt{2} & -1/2 & -\sqrt{3}/2 \end{bmatrix} \times \begin{bmatrix} v^2_{\alpha\beta} & 0 & 0 \\ 0 & v_0 v_\alpha & -v_0 v_\beta \\ 0 & v_0 v_\beta & v_0 v_\alpha \end{bmatrix} \begin{bmatrix} 0 \\ 0 \\ q_{\alpha\beta} \end{bmatrix} \quad (19)$$

$$\begin{bmatrix} i^*_{ca_{fq\_\mathrm{dc}}} \\ i^*_{cb_{fq\_\mathrm{dc}}} \\ i^*_{cc_{fq\_\mathrm{dc}}} \end{bmatrix} = \sqrt{\frac{2}{3}} \times \frac{1}{v_0 v^2_{\alpha\beta}} \begin{bmatrix} 1/\sqrt{2} & 1 & 0 \\ 1/\sqrt{2} & -1/2 & \sqrt{3}/2 \\ 1/\sqrt{2} & -1/2 & -\sqrt{3}/2 \end{bmatrix} \times \begin{bmatrix} v^2_{\alpha\beta} & 0 & 0 \\ 0 & v_0 v_\alpha & -v_0 v_\beta \\ 0 & v_0 v_\beta & v_0 v_\alpha \end{bmatrix} \begin{bmatrix} 0 \\ 0 \\ \Delta Q_{\mathrm{dc}} \end{bmatrix} \quad (20)$$

$$\begin{bmatrix} i^*_{ca_{fp\_\mathrm{dc}}} \\ i^*_{cb_{fp\_\mathrm{dc}}} \\ i^*_{cc_{fp\_\mathrm{dc}}} \end{bmatrix} = \sqrt{\frac{2}{3}} \times \frac{1}{v_0 v^2_{\alpha\beta}} \begin{bmatrix} 1/\sqrt{2} & 1 & 0 \\ 1/\sqrt{2} & -1/2 & \sqrt{3}/2 \\ 1/\sqrt{2} & -1/2 & -\sqrt{3}/2 \end{bmatrix} \times \begin{bmatrix} v^2_{\alpha\beta} & 0 & 0 \\ 0 & v_0 v_\alpha & -v_0 v_\beta \\ 0 & v_0 v_\beta & v_0 v_\alpha \end{bmatrix} \begin{bmatrix} 0 \\ \Delta P_{\mathrm{dc}} \\ 0 \end{bmatrix} \quad (21)$$

Control action in (18). During this period, the dc-link voltage will be self-charging under $I_{cx} > I^*_{cxfq}$ condition. As the dc-link voltage is increased and approaching the reference value, the compensating current tracking ability of the LC-HAPF will be improved gradually, and the control signals ΔQ_{dc} and ΔP_{dc} in (16) and (17) will also be decreased gradually; thus, $i^*_{cx} \approx i_{cx}$ eventually. According to the analysis in Section III, the dc-link voltage will not be affected by the reactive component when $i^{"}_{cx} \approx i_{cx}$. Hence, during this period, the dc-link voltage control signal as active current component will dominate the control action in (18). Therefore, the proposed dc-link voltage control method can be realized as:

- ΔQ_{dc} control signal is used to step change the dc-link voltage under insufficient dc-link voltage that can be effectively applied for start-up process and the adaptive dc-link voltage control;
- ΔP_{dc} control signal is used to maintain the dc-link voltage under sufficient dc-link voltage.

By using the proposed method, the LC-HAPF can compensate the reactive power consumed by the load, and keep the dc-link voltage as its reference one as shown in Figure 9 ($Q_{sxf} \approx 0$ var, $V_{dcU} = V_{dcL} = V^*_{dc}/2 = 30$ V). There-fore, the proposed dc-link voltage control method can effectively control the dc-link voltage without any extra precharging process and lets the LC-HAPF provide dynamic reactive power compensation. Table 2 shows the comparison among the conventional and proposed dc-link voltage control methods error. Since the parameter design of the dc-link voltage controller is not the main theme of this paper, a pure proportional controller with an appropriate value is selected. A limiter is applied to avoid the overflow problem. After that, the final dc-link voltage control reference currents i^*_{cxfq} dc and

Figure 9: Control Process of the Proposed dc-link Voltage Control Method

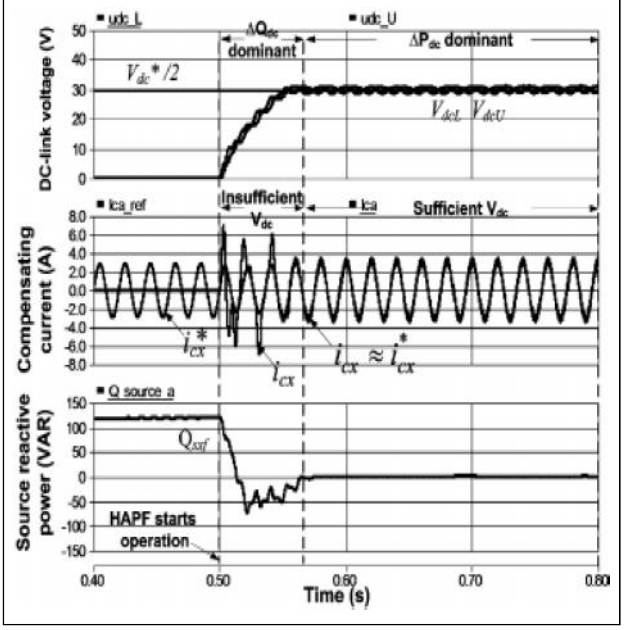

i^*_{cxfp} dc can be calculated, and they will be sent to current PWM control block to perform the dc-link voltage control.

Then, the final reference compensating current i^*_{cx} can be obtained by summing up the i^*_{Lxfq}, i^*_{cxfq} dc, and i^*_{cxfp} dc. Then i^*_{cx} together with compensating current i_{cx} will be sent to the current PWM control part for generating PWM trigger signals to control the power electronic switches of the inverter.

Table 2: Comparison Between Conventional and Proposed dc-Link Control Methods

Functions	DC-link voltage control methods		
	Feedback as active current component [5] – [8], [14] – [18]	Feedback as reactive current component [21]	Proposed
Start-up self-charging	X	O	O
DC-link voltage control	O*	O	O
Adaptive dc-link voltage control [20]	O*	O	O
Dynamic reactive power compensation	O*	X	O

Note: O – function, X – failure, O* – conditionally can work under sufficient current tracking ability.

SIMULATION RESULTS

Figure 10: Circuit Diagram

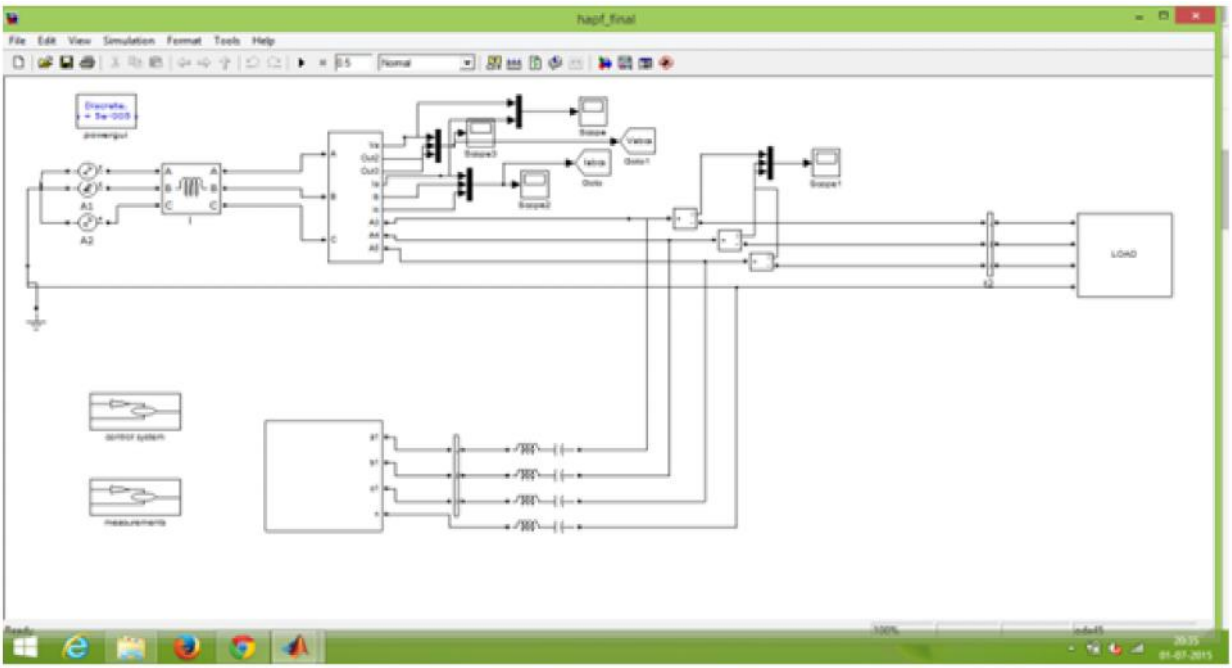

Figure 11: Input Voltage and Current

Figure 12: Load Currents

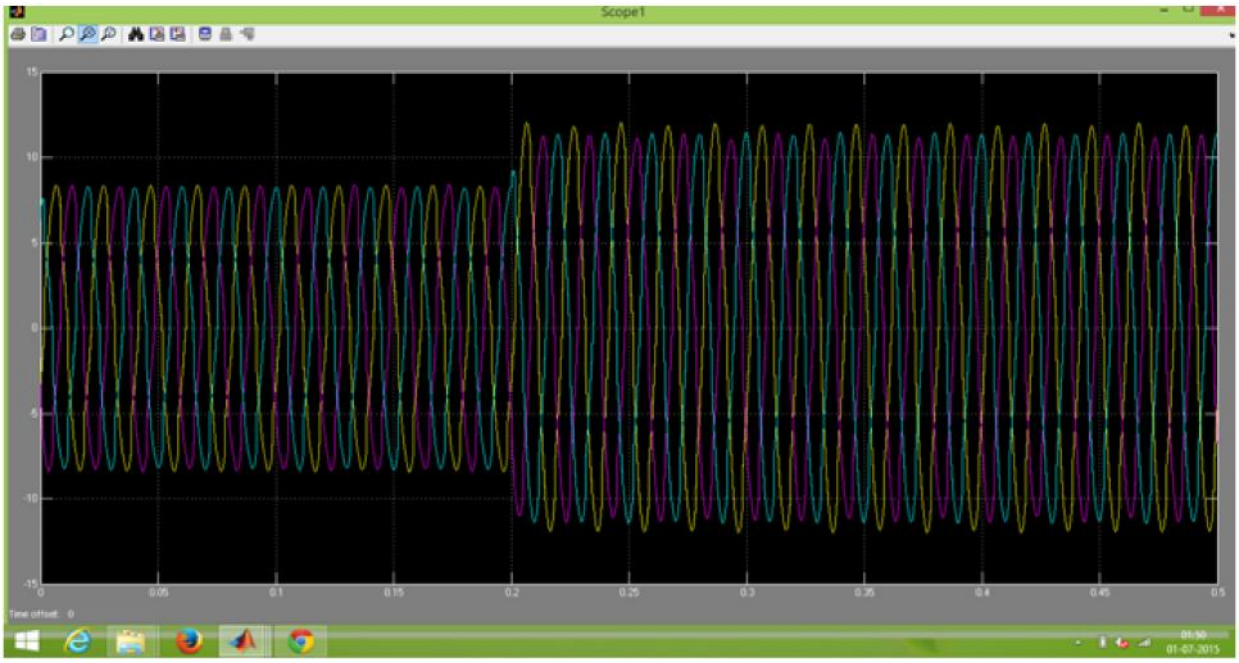

CONCLUSION

The shunt APF is implemented with three-phase supply controlled with voltage source inverter and is connected at the point of common coupling for filtering the current harmonics. The VSI switching signals are derived from hysteresis band current controller. The hysteresis controller changes the bandwidth based on instantaneous compensation current variation. The proposed controller based shunt active power filter performs perfectly for mitigate the harmonics Through the proposed dc-link voltage control method:

1) The *LC*-HAPF can achieve start-up dc-link self-charging function;
2) The dc-link voltage of the *LC*-HAPF can be controlled as its reference level;
3) The *LC*-HAPF can provide dynamic reactive power compensation;
4) The adaptive dc-link voltage reference control can be implemented.

Finally, simulation results of the three-phase four-wire center-spilt *LC*-HAPF under dynamic reactive power compensation application are presented to verify all discussions and analysis, and also show the effectiveness of the proposed dc-link voltage control method.

REFERENCES

1. Akagi H (1996), “New Trends in Active Filters for Power Conditioning”, *IEEE Trans. Ind. Appl.*, Vol. 32, No. 6, pp. 1312-1322.
2. Aredes M, Hafner J and Heumann K (1997), “Three-Phase Four-Wire Shunt Active Filter Control Strategies”, *IEEE Trans. Power Electron.*, Vol. 12, No. 2, pp. 311-318.
3. Cui X-X, Lam C-S and Dai N-Y (2011),

"Study on dc Voltage Control of Hybrid Active Power Filters", in *Proc. 6th IEEE Conf. Ind. Electron. Appl. (ICIEA)*, June, pp. 856-861.

4. Duarte L H S and Alves M F (2002), "The Degradation of Power Capacitors Under the Influence of Harmonics", in *Proc. IEEE 10th Int. Conf. Harmonics Quality Power*, Vol. 1, October, pp. 334-339.
5. Fujita H and Akagi H (1991), "A Practical Approach to Harmonic Compensation in Power Systems—Series Connection of Passive and Active Filters", *IEEE Trans. Ind. Appl.*, Vol. 27, No. 6, pp. 1020-1025.
6. Fujita H, Yamasaki T and Akagi H (2000), "A Hybrid Active Filter for Damping of Harmonic Resonance in Industrial Power Systems", *IEEE Trans. Power Electron.*, Vol. 15, No. 2, pp. 215-222.
7. Inzunza R and Akagi H (2005), "A 6.6-kV Transformerless Shunt Hybrid Active Filter for Installation on a Power Distribution System", *IEEE Trans. Power Electron.*, Vol. 20, No. 4, pp. 893-900.
8. Jou H-L, Wu K-D, Wu J-C, Li C-H and Huang M-S (2008), "Novel Power Converter Topology for Three Phase Four-Wire Hybrid Power Filter", *IET Power Electron.*, Vol. 1, pp. 164-173.
9. Lam C-S, Choi W-H, Wong M-C and Han Y-D (2012), "Adaptive dc-link Voltage Controlled Hybrid Active Power Filters for Reactive Power Compensation", *IEEE Trans. Power Electron.*, Vol. 27, No. 4, pp. 1758-1772.
10. Lam C-S, Wong M-C and Han Y-D (2008), "Voltage Swell and Overvoltage Compensation with Unidirectional Power Flow Controlled Dynamic Voltage Restorer", *IEEE Trans. Power Del.*, Vol. 23, No. 4, pp. 2513-2521.
11. Luo A, Shuai Z K, Shen Z J, Zhu W J and Xu X Y (2009b), "Design Considerations for Maintaining dc-side Voltage of Hybrid Active Power Filter with Injection Circuit", *IEEE Trans. Power Electron.*, Vol. 24, No. 1, pp. 75-84.
12. Luo A, Tang C, Shuai Z K, Zhao W, Rong F and Zhou K (2009c), "A Novel Three-Phase Hybrid Active Power Filter with a Series Resonance Circuit Tuned at the Fundamental Frequency", *IEEE Trans. Ind. Electron.*, Vol. 56, No. 7, pp. 2431-2440.
13. Luo A, Zhao W, Deng X, Shen Z J andPeng J-C (2009a), "Dividing Frequency Control of Hybrid Active Power Filter with Multi-injection Branches Using Improved $i_p - i_q$ Algorithm", *IEEE Trans. Power Electron.*, Vol. 24, No. 10, pp. 2396-2405.
14. Park S, Sung J-H and Nam K (1999), "A Newparallel Hybrid Filter Configuration Minimizing Active Filter Size", in *Proc. IEEE 30th Annu. Power Electron. Spec. Conf. (PESC)*, Vol. 1, pp. 400-405.
15. Peng F Z, Akagi H and Nabae A (1990), "A New Approach to Harmonic Compensation in Power Systems—A Combined System of Shunt Passive and Series Active Filters", *IEEE Trans. Ind. Appl.*, Vol. 26, No. 6, pp. 983-990.
16. Rahmani S, Hamadi A, Mendalek N and Al-Haddad K (2009), "A New Control

Technique for Three-Phase Shunt Hybrid Power Filter", *IEEE Trans. Ind. Electron.*, Vol. 56, No. 8, pp. 2904-2915.

17. Rivas D, Moran L, Dixon J W and Espinoza J R (2003), "Improving Passive Filter Compensation Performance with Active Techniques", *IEEE Trans. Ind. Electron.*, Vol. 50, No. 1, pp. 161-170.
18. Salmerón P and Litrán S P (2010), "A Control Strategy for Hybrid Power Filter to Compensate Four-Wires Three-Phase Systems", *IEEE Trans. Power Electron.*, Vol. 25, No. 7, pp. 1923-1931.
19. Senini S T and Wolfs P J (2002), "Systematic Identification and Review of Hybrid Active Filter Topologies", in *Proc. IEEE 33rd Annu. Power Electron. Spec. Conf. (PESC)*, Vol. 1, pp. 394-399.
20. Singh B and Verma V (2005), "An Indirect Current Control of Hybrid Power Filter for Varying Loads", *IEEE Trans. Power Del.*, Vol. 21, No. 1, pp. 178-184.
21. Srianthumrong S and Akagi H (2003), "A Medium-Voltage Transformerless ac/dc Power Conversion System Consisting of a Diode Rectifier and a Shunt Hybrid Filter", *IEEE Trans. Ind. Appl.*, Vol. 39, No. 3, pp. 874-882.
22. Subjek J S and Mcquilkin J S (1990), "Harmonics-Causes, Effects, Measurements and Analysis", *IEEE Trans. Ind. Electron.*, Vol. 26, No. 6, pp. 1034-1042.
23. Tai S-U, Wong M-C, Dong M-C and Han Y-D (2007), "Some Findings on Harmonic Measurement in Macao", in *Proc. 7th Int. Conf. Power Electron. Drive Syst. (PEDS)*, pp. 405-410.
24. Tangtheerajaroonwong W, Hatada T, Wada K and Akagi H (2007), "Design and Performance of a Transformerless Shunt Hybrid Filter Integrated into a Three-Phase Diode Rectifier", *IEEE Trans. Power Electron.*, Vol. 22, No. 5, pp. 1882-1889.